

- Bergh, S. van den. 1963, *J. Roy. Astron. Soc. Canada* 57, 63.  
 ——. 1964, *Astrophys. J. Suppl.* 9, 65.  
 Fernie, J. D. 1963, *Astron. J.* 68, 780.  
 Gaposchkin, S. 1962a, *ibid.* 67, 334.  
 ——. 1962a, *ibid.* 67, 358.  
 Harris, D. L. 1956, *Astrophys. J.* 124, 665.  
 Hayashi, C., and Cameron, R. C. 1962, *ibid.* 136, 166.  
 Hoag, A. A., Johnson, H. L., Iriate, B., Mitchell, R. I., Hallam, K. L., and Sharpless, S. 1961, *Publ. U. S. Naval Obs.* 17, pt. 7.  
 Johnson, H. L. 1958, *Lowell Obs. Bull.* 4, 37.  
 Johnson, H. L., and Harris, D. L. 1954, *Astrophys. J.* 120, 196.  
 Johnson, H. L., and Hiltner, W. A. 1956, *ibid.* 123, 267.  
 Kron, G. E., and Mayall, N. U. 1960, *Astron. J.* 65, 581.  
 Marlborough, J. M. 1964, *ibid.* 69, 215.  
 Oort, J. H. 1960, *Bull. Astron. Inst. Neth.* 15, 45 (No. 494).  
 Sandage, A. R. 1964, *Astrophys. J.* 139, 442.  
 Sandage, A. R., and Eggen, O. J. 1959, *Monthly Notices Roy. Astron. Soc.* 119, 278.  
 Sandage, A. R., and Smith, L. L. 1963, *Astrophys. J.* 137, 1057.  
 Schmidt, M. 1959, *ibid.* 129, 243.  
 Wildey, R. L., Burbidge, E. M., Sandage, A. R., and Burbidge, G. R. 1962, *Astrophys. J.* 135, 94.

## Detailed Photoelectric Photometry of the Moon\*

ROBERT L. WILDEY

*Division of Geological Sciences and Mount Wilson and Palomar Observatories,  
 California Institute of Technology and Carnegie Institution of Washington*

AND

HOWARD A. POHN

*Division of Geological Sciences, California Institute of Technology*

(Received 1 June 1964)

A number of lunar features extending over a range in both morphological type and selenographic coordinates have been measured photoelectrically in  $U$ ,  $B$ , and  $V$ . The observations extend from  $28^\circ$  in phase angle before full moon to  $28^\circ$  after. They have been measured during several lunations so that a continuous brightness versus phase curve is precluded by the differences in libration. This is a necessary technique for obtaining that component of brightness variation that arises from variations in the local altitude of the earth above the lunar horizon. The nature of the photometric function corresponding to the average behavior of nearly all the observations has been investigated and found to substantiate the previous conclusions, based on an analysis of photographic observations according to an entirely different approach, that the functional dependence on  $(g, A\odot, A\oplus)$  can be well approximated by a dependence on  $(g, \alpha)$ . A numerical comparison with earlier photographic results has not been made. Deviations from the average photometric function have been correlated with stratigraphic class (hence, probably, age). Correlations of geometrically normalized brightness with stratigraphy, characteristic slope, and color index are presented. A conjectural hypothesis relating these correlations to the evolution of the lunar surface is offered for further study.

### I. INTRODUCTION

THE history of lunar photometry has been recently reviewed by Minnaert (1961) and by Fessenkov (1961). The most striking characteristic of this history is that, although photoelectric observations of the total lunar flux with adequate phase coverage were carried out as early as 1933 (Rougier 1933; Bullrich 1948), the high-resolution photometric observations of detailed brightnesses have been restricted to pure photographic techniques. Excepted are observations of lunar color indices (van den Bergh 1962) and eclipse observations (Barbier 1961).

It is known that in stellar photometry the development of magnitude-color systems by pure photography leads to systematic errors of considerable size as may be seen by comparing the modern photoelectric magnitudes with the listings in old star catalogues. Even photometry by photographic transfers from selected

areas, whose photometric sequences may be assumed, can lead to relative scale and zero point errors of nearly 0.3 mag., though done with meticulous care. Of course the seeing component of these systematic errors is not so severe for the detail of extended celestial bodies as it is for entire stellar images. Nevertheless, the extension of photoelectric photometry into the investigation of the detailed photometric function of the moon, and the testing of this function's possible correlation with color, normal albedo, and geomorphology, seems advised.

The significance of precise detailed lunar photometry is manifold. Not only is the resulting photometric function a constraint which must be satisfied by physical models, be they based on the scattering, according to some phase function, by the particulate matter in a "dust" atmosphere, or the unresolved shadows cast by microtopographic relief, but the function is also the key to the insolation function in the heat flow equation (presently being investigated by Watson) which leads to a comparison of theory and observation with regard to the lunar infrared emission. In addition,

\* Contribution No. 1254 of the Division of Geological Sciences, California Institute of Technology, Pasadena, California.

the variation of the parameters of the photometric function over the lunar surface, or departures from uniqueness of the functional form itself, are potentially useful geologic mapping tools.

The photographic observations of Fedoretz (1952), augmented by the later work of van Diggelen (1959), cover extensively the lunar surface over a wide range in phase angle. Several investigators have pointed out a curious phenomenon which is implicit in these observations and which is responsible for the concentration of the present observations near full moon. The maximum brightness does not always occur at minimum phase. The maximum light of the brighter features exhibits a phase lag apparently uncorrelated with selenographic coordinates. This phase lag appears to be an increasing function of normal albedo, amounting to as much as  $13^\circ$  for the brightest rayed craters. Such a phenomenon, not easily understood, seemed a proper candidate for photoelectric investigation.

The present observations have been made on the *UBV* system (Johnson and Morgan 1953). They may thus be converted to absolute specific intensities ( $W/cm^2/\text{\AA}/sr$ ), at the effective wavelengths of the *UBV* system, using the calibration of Willstrop (1960). They cover the range in phase angle from  $28^\circ$  before minimum phase to  $28^\circ$  after.

## II. OBSERVATIONS

The observations were collected on three nights in April 1962, one in May, one in June, three in July, one in August, three in September, two in December, and one night in January 1963 using the Newtonian focus of the 60-in. telescope of the Mt. Wilson Observatory. The photometer employed a dry-ice refrigerated 1P21 photomultiplier whose signal was fed into a General Radio dc amplifier and read out on a Brown strip-chart



FIG. 1. Finding chart for lunar features investigated photoelectrically in the present study.

recorder. The filters used were 2.0 mm Corning 9863 for *U*, 1.3 mm Schott GG13 plus 0.7 mm BG12 for *B*, and 2.0 mm GG11 for *V*. Each nights observations were usually reduced separately. The atmospheric extinction correction and the transformation to the *UBV* system were accomplished using from 20 to 40 standard stars and the Fortran program of Abel.

The smallest focal plane diaphragm aperture (10.8 sec of arc) of the Peoples photometer base was used. In order to keep from shocking the 1P21 and to ensure against the nonlinearity associated with space-charge limited operation in the upper dynode stages, from 5 to 7.5 mag. of Wratten No. 96 neutral-density gelatin filter were employed. The attenuation used depended upon the run, and was used on various occasions in conjunction with no mirror diaphragm, the 32-in. diaphragm, and the 18-in. off-axis diaphragm, and a lowering on one occasion of the total dynode voltage drop from 900 to 700 V. The coefficient in the *B-V* color equation was the only significantly not unity (consistently about 1.3). Nevertheless the plots of the residuals of the standard stars against *B-V* always appeared random. Our average *B-V* for the maria points are in good agreement with van den Bergh's.

The degree of instrumental polarization introduced by the Newtonian flat mirror is 3%. The plane of the maximum electric vector, for initially unpolarized light, contains the local segment of the declination circle passing through the moon's neighborhood. The observations have not been corrected for this effect, which is too small to alter the conclusions reached in the present paper.

Twenty-five lunar features were chosen with widespread coverage of the lunar disk and including the morphological classes of maria, bright straight-ray craters, "aged"-ray craters, and nonrayed craters. These features are shown in Fig. 1. A significant source of error in their photometry, in the case of small contrasty objects, can be the lack of a satisfactory lunar rate on the 60-in. telescope. An automatic, periodic right ascension-declination relay-pulsing device was used, which was not completely stable and could not be set at a suitable pulse-frequency to pulse-width ratio because of the prohibitive rate of relay malfunction. The importance of poor tracking as a source of error can be shown by plotting probable photometric errors for small bright craters versus the ratio of the diameter of the crater image to that of the focal plane aperture. No noticeable correlation was found.

The *upper bound* of the general random error can be seen in the histograms of Fig. 2, which appear to follow normal distributions. Of course, insofar as the assumption that no component of the dispersion in color indices is cosmic remains invalid, the observational error is smaller than the histograms indicate. It is noted that the histograms of the *U-B* observations of separate runs are much narrower than the range of the run-to-run variation of the position of their maxima. Graphical

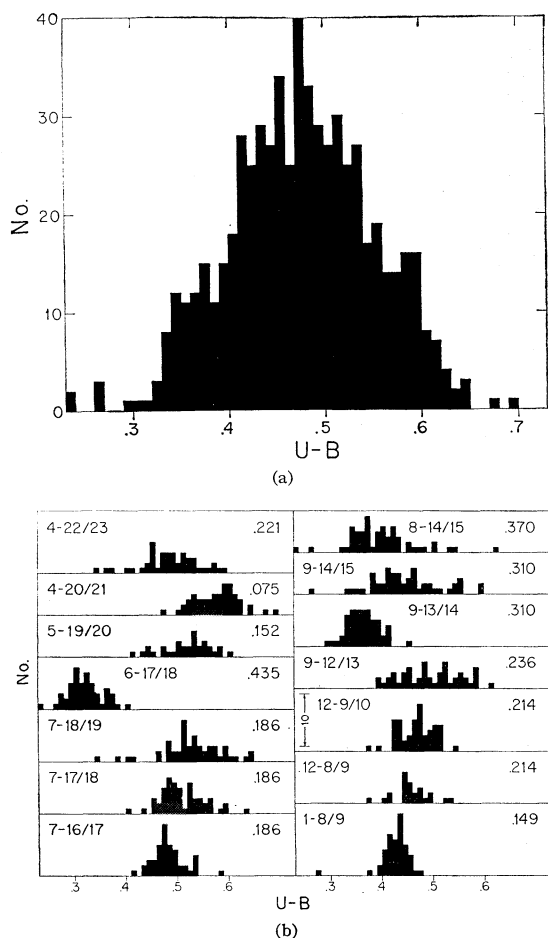


FIG. 2. (a) Histogram showing frequency distribution of all measurements of  $U-B$ . (b) Histograms showing frequency distribution of  $U-B$  measurements for each observing night. Numbers on left are local dates of observations. Numbers on right are  $U-B$  extinction coefficients determined for the night.

attempts were made to correlate the average  $U-B$  of a given night's lunar observations with (1) the coefficients found in the color equations tying that night to the  $UBV$  system, and also (2) the average  $U-B$  and  $B-V$  of the standard stars used to obtain the color equations for that night. It was felt that the nonneutral character of the Wratten 96 filter might have invalidated the color equation for  $U-B$  because of the Balmer jump. No correlation was found. Correlation with solar flares and geomagnetic storms, when examined, *vaguely* suggested itself. Correlation with the extinction coefficient found nightly in the over-all least-squares reduction of deflections to  $U$ ,  $B$ , and  $V$ , was, however, very good. Furthermore, reading the mean graphical relation so derived at the standard extinction coefficient yields a  $U-B$  equal to the over-all average. This phenomenon is probably due to higher than first-order terms in  $\sec z$  being present in the  $U-B$  extinction function as a result of strongly wavelength dependent atmospheric absorption across the  $U$  band.

The formal probable error of a single measurement is computed to be 0.016 mag. in  $V$ , 0.031 in  $B-V$ , and 0.023 in  $U-B$ , determined from periodic double observations.

The observations are tabulated in Table I. Identification of object numbers is shown in Table II. Topocentric effects on phase angle are neglected.

### III. RESULTS

#### A. Photometric Function

Figure 3 shows the brightness [ $V$  of one (arc-sec) $^2$ ] versus phase for each of the objects of the present study. Because the observations are collected over many lunations, for each of which the libration is different, some cosmic scatter is present, i.e., the elevation angles of the sun and earth are not reproduced for a given phase angle. This effect is illustrated in Fig. 3(e). In Figs. 3(a)-(d) points before minimum phase are shown by closed circles and points after by open circles. It is clear that *maximum brightness* is always achieved at *minimum phase*. It is also clear that the deviation between the waxing and waning curves is greater for objects at extreme selenographic longitudes—a manifestation of the fact that the phase angle is not the only degree of freedom in which the photometric function is nondegenerate.

The curves of Fig. 3 are approximately linear in the range of phase angle from  $5^\circ$  to  $25^\circ$ . It is thus a good range in which to evaluate the total derivative  $dV/dg$  ( $g$  is the phase angle). For each observation of the present study the elevation angles of the sun and earth ( $A_\odot$  and  $A_\oplus$ ) together with the phase angle and the brightness longitude  $\alpha$  [defined as the angle, in the same plane as the phase angle, equal to the projection of the complement of  $A_\oplus$ —see also Eimer (1963) and Wildey (1963)] were evaluated using a Fortran program by Watson and Wildey.

Values of  $\Delta A_\odot/\Delta g$ ,  $\Delta A_\oplus/\Delta g$ , and  $\Delta\alpha/\Delta g$  were computed from paired observations and the plots of  $\Delta V/\Delta g$  against them are shown in Figs. 4, 5, and 6, respectively. There appears to be less scatter in the plot of the data against  $\Delta\alpha/\Delta g$  than against  $\Delta A_\odot/\Delta g$ . The very extreme scattering points in both plots are cases where the object was partially shadowed while being observed (suggesting that if the photometric function is a micro-shadowing phenomenon then the microtopography is far from a scaled down version of the macrotopography).

A least-squares solution, beginning with all the observations, was made to two simply assumed forms of the photometric function. Following each solution the residuals of observed  $\Delta V/\Delta g$ 's compared to predictions from the derived formulas were examined and rejected if greater than 3.5 times the average. Both solutions rejected the same 15 data and the final results were

$$\Delta V = 0.0237\Delta g - 0.00638\Delta A_\odot + 0.0136\Delta A_\oplus \quad (1)$$

TABLE I. Observational results.

Object	Date	UT	V	B-V	U-B	g	$A_{\odot}$	$A_{\oplus}$	$\alpha$
1	4-20-62	5.8	2.84	0.87	0.57	5.4°	29.8°	29.7°	3.5°
2	4-20-62	6.1	3.74	0.82	0.55	5.5	36.7	34.3	34.1
3	4-20-62	6.2	2.88	0.83	0.61	5.5	43.7	38.6	48.9
4	4-20-62	7.7	3.41	0.90	0.57	5.8	57.6	53.0	31.5
7	4-20-62	7.3	3.13	0.86	0.58	5.8	65.9	67.5	- 3.8
10	4-20-62	7.3	2.91	0.89	0.58	5.8	72.4	66.8	22.8
11	4-20-62	7.4	3.30	0.84	0.51	5.8	73.9	68.2	21.3
12	4-20-62	7.5	3.36	0.91	0.58	5.9	69.2	73.5	-11.0
13	4-20-62	7.5	2.70	0.84	0.55	5.9	49.3	53.8	-28.6
14	4-20-62	7.6	2.97	0.86	0.51	5.9	69.8	74.8	-12.2
15	4-20-62	7.6	3.62	0.81	0.50	5.9	71.4	68.0	14.8
16	4-20-62	7.7	3.24	0.85	0.55	5.9	53.6	49.3	32.7
1	4-21-62	6.7	2.79	0.94	0.64	15.1	40.8	30.5	50.9
2	4-21-62	6.8	4.01	0.84	0.55	15.1	49.2	35.1	53.3
3	4-21-62	6.9	3.11	0.62	0.54	15.2	53.1	39.1	49.0
4	4-21-62	7.0	3.58	0.86	0.60	15.2	68.8	53.7	36.2
7	4-21-62	7.2	3.44	0.95	0.60	15.3	70.4	68.2	10.8
10	4-21-62	7.2	3.23	0.86	0.57	15.3	78.2	67.2	20.3
11	4-21-62	7.3	3.62	0.84	0.59	15.4	72.7	68.4	13.4
12	4-21-62	7.4	3.77	0.88	0.61	15.4	66.7	73.8	- 1.6
13	4-21-62	7.4	3.08	0.83	0.60	15.4	48.6	54.1	- 8.0
14	4-21-62	7.4	3.42	0.87	0.62	15.4	65.5	75.0	- 4.7
15	4-21-62	7.5	4.10	0.85	0.55	15.4	63.4	67.7	0.6
16	4-21-62	7.6	3.61	0.85	0.59	15.5	49.4	49.1	8.6
17	4-21-62	7.6	3.14	0.87	0.60	15.5	36.6	32.1	31.0
30	4-21-62	8.5	3.94	0.91	0.52	15.9	14.2	9.4	63.4
18	4-21-62	7.7	3.54	0.89	0.59	15.5	29.5	30.1	3.9
19	4-21-62	7.8	3.72	0.92	0.61	15.6	58.4	65.5	- 5.8
20	4-21-62	7.9	3.33	0.86	0.61	15.6	60.3	73.0	-11.6
21	4-21-62	8.0	3.60	0.82	0.67	15.7	52.9	66.1	-18.6
22	4-21-62	8.1	3.57	0.89	0.60	15.7	42.6	58.2	-31.6
23	4-21-62	8.1	3.44	0.86	0.61	15.7	40.0	55.6	-34.1
24	4-21-62	8.2	4.23	0.88	0.56	15.8	33.9	42.3	-26.3
26	4-21-62	8.3	3.32	0.89	0.62	15.8	22.3	34.5	-47.0
27	4-21-62	8.3	4.66	0.82		15.8	8.9	22.2	-63.7
28	4-21-62	8.4	4.04	0.86	0.60	15.9	23.4	37.5	-48.5
29	4-21-62	8.4	3.46	0.88	0.64	15.9	16.3	31.6	-57.4
1	4-21-62	9.3	2.92	0.85	0.53	16.2	41.9	30.6	51.5
2	4-21-62	9.3	4.07	0.84	0.54	16.2	50.2	35.2	53.5
3	4-21-62	9.4	3.03	0.80	0.57	16.3	54.0	39.2	48.8
4	4-21-62	9.4	3.52	0.90	0.56	16.3	69.9	53.8	36.1
7	4-21-62	9.5	3.55	0.88	0.57	16.3	70.5	68.2	11.2
10	4-21-62	9.6	3.33	0.86	0.58	16.4	78.3	67.2	19.9
11	4-21-62	9.7	3.74	0.86	0.57	16.4	72.1	68.4	12.9
12	4-21-62	9.7	3.80	0.89	0.59	16.4	66.2	73.8	- 1.3
13	4-21-62	9.9	3.09	0.85	0.58	16.5	48.4	54.1	- 7.0
14	4-21-62	9.9	3.55	0.89	0.60	16.5	64.8	74.9	- 4.3
15	4-21-62	10.0	4.17	0.87	0.54	16.6	62.4	67.6	- 0.1
16	4-21-62	10.0	3.71	0.89	0.59	16.6	48.8	49.1	7.4
17	4-21-62	10.1	3.09	0.88	0.58	16.6	36.5	37.0	29.3
30	4-21-62	11.0	3.96	0.90	0.52	17.0	14.2	9.4	61.7
18	4-21-62	10.2	3.50	0.93	0.62	16.7	28.9	30.0	1.4
19	4-21-62	10.3	3.55	0.77	0.59	16.7	57.3	65.5	- 6.5
20	4-21-62	10.3	3.40	0.91	0.53	16.7	59.1	73.0	-11.9
21	4-21-62	10.4	3.79	0.86	0.50	16.8	51.7	66.1	-19.0
22	4-21-62	10.4	3.66	0.91	0.51	16.8	41.5	58.2	-31.7
23	4-21-62	10.5	3.62	0.95	0.53	16.8	38.9	55.6	-34.2
24	4-21-62	10.5	4.34	0.86	0.47	16.8	32.9	42.2	-27.3
26	4-21-62	10.6	3.52	0.81	0.55	16.8	21.2	34.5	-47.6
27	4-21-62	10.6	4.64	0.90	0.51	16.8	7.8	22.2	-64.1
28	4-21-62	10.7	4.13	0.92	0.52	16.9	22.3	37.5	-48.9
29	4-21-62	10.7	3.65	0.92	0.53	16.9	15.3	31.6	-57.2
1	4-22-62	7.1	2.99	0.89	0.59	26.4	50.9	31.0	53.9
2	4-22-62	7.2	4.14	0.90	0.53	26.4	61.6	35.7	53.9
3	4-22-62	7.3	2.90	0.88	0.55	26.5	60.5	39.7	46.3
4	4-22-62	7.4	3.53	0.86	0.48	26.5	78.4	54.3	34.8
7	4-22-62	7.5	3.61	0.93	0.52	26.6	68.3	68.5	13.1
10	4-22-62	7.6	3.50	0.95	0.52	26.6	73.7	67.7	17.7
11	4-22-62	7.6	3.97	0.95	0.45	26.6	64.8	68.7	9.8
12	4-22-62	7.7	3.71	0.86	0.57	26.7	59.4	73.8	0.4
13	4-22-62	7.7	3.28	0.90	0.51	26.7	45.2	54.0	- 2.1

## PHOTOELECTRIC PHOTOMETRY OF MOON

623

TABLE I (continued)

Object	Date	UT	V	B-V	U-B	g	A <sub>☉</sub>	A <sub>⊕</sub>	α
14	4-22-62	7.9	3.54	0.94	0.49	26.8°	57.0°	74.7°	- 3.0°
15	4-22-62	7.9	4.25	0.87	0.49	26.8	53.0	67.1	- 3.8
16	4-22-62	8.0	3.90	0.86	0.44	26.8	42.6	49.2	0.2
17	4-22-62	8.1	3.35	0.87	0.48	26.9	34.0	32.3	19.0
30	4-22-62	8.0	4.26	0.90	0.44	26.8	13.3	9.6	47.3
18	4-22-62	8.2	3.85	0.88	0.45	26.9	23.4	30.1	-12.2
19	4-22-62	8.3	3.61	0.86	0.50	27.0	47.3	65.4	-10.3
20	4-22-62	8.3	3.55	0.90	0.45	27.0	48.0	72.6	-14.0
21	4-22-62	8.3	3.69	0.83	0.41	27.0°	40.6°	65.7°	-21.3°
22	4-22-62	8.4	3.94	0.91	0.49	27.0	30.6	57.6	-32.4
23	4-22-62	8.4	3.79	0.91	0.49	27.0	28.0	55.0	-35.0
24	4-22-62	8.5	4.74	0.86	0.43	27.1	23.4	42.0	-33.2
26	4-22-62	8.7	4.51	1.09	0.46	27.2	10.5	34.0	-51.0
28	4-22-62	8.7	5.03	0.84	0.48	27.2	11.2	37.0	-51.2
1	4-22-62	10.4	3.13	0.85	0.51	28.0	52.2	31.0	54.1
2	4-22-62	10.4	4.24	0.87	0.48	28.0	63.2	35.8	53.8
3	4-22-62								
4	4-22-62	10.5	3.53	0.99	0.51	28.0	79.2	54.4	34.7
7	4-22-62	10.6	3.97	0.83	0.37	28.1	67.5	68.5	13.3
10	4-22-62	10.6	3.55	0.96	0.54	28.1	72.6	67.8	17.5
11	4-22-62	10.7	4.11	0.90	0.36	28.1	63.5	68.8	9.4
12	4-22-62	11.0	4.03	0.94	0.46	28.3	58.2	73.7	0.5
13	4-22-62	11.0	3.33	0.90	0.47	28.3	44.5	53.9	- 1.5
14	4-22-62	11.1	3.78	0.91	0.51	28.3	55.7	74.7	- 2.8
15	4-22-62	11.1	4.36	0.88	0.40	28.3	51.5	67.7	- 4.1
16	4-22-62	11.1	4.00	0.90	0.45	28.3	41.6	49.2	- 0.5
17	4-22-62	11.2	3.40	0.95	0.52	28.4	33.6	32.4	17.9
30	4-22-62	11.2	4.23	0.96	0.34	28.8	13.1	9.7	44.4
18	4-22-62	11.2	3.88	1.03	0.51	28.4	22.6	30.1	-13.4
19	4-22-62	11.4	3.93	0.96	0.57	28.5	45.9	65.4	-10.7
20	4-22-62	11.5	3.77	0.91	0.47	28.5	46.3	72.6	-14.2
21	4-22-62	11.6	3.69	0.99	0.58	28.5	39.0	65.6	-21.5
22	4-22-62	11.8	3.85	0.99	0.53	28.6	28.9	57.5	-32.4
23	4-22-62	11.8	4.40	0.96	0.47	28.6	26.3	54.9	-35.0
24	4-22-62	11.9	4.85	0.93	0.45	28.7	21.9	42.0	-33.7
26	4-22-62	11.9	4.47	1.04	0.56	28.7	9.0	34.0	-51.3
28	4-22-62	12.1	4.94	1.02	0.55	28.8	9.5	36.9	-51.4
1	5-20-62	6.8	2.84	0.83	0.55	9.2	35.7	30.5	45.4
2	5-20-62	6.9	4.07	0.83	0.54	9.3	43.3	35.3	51.0
3	5-20-62	6.9	1.99	0.82	0.58	9.3	48.8	39.7	49.8
4	5-20-62	7.0	2.33	0.88	0.55	9.3	63.4	54.1	35.7
7	5-20-62	7.0	2.45	0.86	0.52	9.3	68.8	67.9	7.0
10	5-20-62	7.1	3.22	0.88	0.53	9.4	76.3	67.8	21.2
11	5-20-62	7.1	3.66	0.95	0.47	9.4	74.4	69.0	15.5
12	5-22-62	7.2	3.48	0.87	0.52	9.4	68.7	73.2	- 4.7
13	5-20-62	7.2	3.06	0.86	0.53	9.4	49.3	53.5	-14.7
14	5-20-62	7.3	3.27	0.83	0.56	9.5	68.3	74.3	- 7.5
15	5-20-62	7.4	4.07	0.84	0.44	9.5	67.8	68.2	3.8
16	5-20-62	7.4	3.60	0.87	0.50	9.5	51.8	49.7	15.3
17	5-20-62	7.5	3.07	0.85	0.58	9.5	37.2	32.7	38.7
30	5-20-62	7.6	3.97	0.93	0.45	9.6°	14.5°	10.0°	69.7°
18	5-20-62	7.6	3.50	0.89	0.53	9.6	32.0	30.6	17.7
19	5-20-62	7.7	3.49	0.84	0.50	9.6	63.4	65.9	- 2.4
20	5-20-62	7.7	3.27	0.89	0.55	9.6	66.3	73.2	- 9.9
21	5-20-62	7.8	3.30	0.82	0.51	9.7	58.9	66.2	-16.5
22	5-20-62	7.8	3.38	0.85	0.50	9.7	48.5	57.9	-31.2
23	5-20-62	7.9	3.74	0.92	0.51	9.7	45.9	55.4	-33.6
24	5-20-62	7.9	4.18	0.85	0.44	9.7	38.9	42.6	-19.0
26	5-20-62	8.0	3.10	0.92	0.60	9.8	28.1	34.6	-42.6
27	5-20-62	8.0	4.50	0.83	0.43	9.8	14.9	22.2	-61.0
28	5-20-62	8.1	3.87	0.87	0.48	9.8	29.5	37.5	-45.9
29	5-20-62	8.1	3.08	0.89	0.47	9.8	21.4	31.1	-58.6
1	6-18-62	8.4	2.69	0.83	0.35	4.7	31.2	29.7	32.4
2	6-18-62	8.4	3.78	0.80	0.26	4.7	38.4	35.2	45.2
3	6-18-62	8.5	2.73	0.92	0.34	4.7	45.3	40.6	49.3
4	6-18-62	8.5	3.16	0.82	0.36	4.7	58.9	54.6	33.3
7	6-18-62	8.6	3.25	0.83	0.38	4.7	66.2	66.6	0.4
10	6-18-62	8.6	3.08	0.83	0.36	4.7	73.6	68.8	21.2
11	6-18-62	8.8	3.39	0.81	0.31	4.8	74.6	70.5	17.2
12	6-18-62	8.9	3.55	0.81	0.29	4.9	68.8	71.6	- 9.3
13	6-18-62	8.9	2.82	0.85	0.37	4.9	49.0	51.8	-23.6

TABLE I (continued)

Object	Date	UT	V	B-V	U-B	g	A <sub>⊙</sub>	A <sub>⊕</sub>	α
14	6-18-62	8.9	3.01	0.82	0.34	4.9°	69.2°	72.7°	-11.4°
15	6-18-62	9.0	3.75	0.84	0.30	4.9	70.1	69.8	7.6
16	6-18-62	9.0	3.39	0.83	0.32	4.9	53.7	51.3	22.7
17	6-18-62	9.1	2.82	0.85	0.36	4.9	37.7	34.4	45.2
30	6-18-62	9.1	3.71	0.83	0.32	4.9	14.9	11.7	72.6
18	6-18-62	9.2	3.18	0.85	0.31	5.0	34.1	32.3	31.7
19	6-18-62	9.3	3.12	0.77	0.32	5.0	67.3	67.4	2.0
20	6-18-62	9.3	3.09	0.84	0.33	5.0	71.1	74.0	- 7.7
21	6-18-62	9.4	3.10	0.82	0.34	5.0	63.8	66.9	-13.5
22	6-18-62	9.4	3.00	0.85	0.31	5.0	53.1	57.7	-30.0
23	6-18-62	9.4	3.38	0.88	0.28	5.0	50.6	55.2	-32.2
24	6-18-62	9.5	3.74	0.82	0.36	5.1	43.0	43.9	- 8.3
26	6-18-62	9.6	2.83	0.78	0.40	5.1	32.8	35.5	-34.5
27	6-18-62	9.6	3.85	0.82	0.30	5.1	20.0	22.8	-55.1
28	6-18-62	9.6	3.62	0.83	0.33	5.1	34.4	38.0	-40.7
29	6-18-62	9.7	2.78	0.78	0.27	5.2	25.2	30.3	-59.6
1	7-17-62	6.1	2.74	0.81	0.39	3.1	25.3	28.4	-61.2
2	7-17-62	6.2	3.92	0.78	0.44	3.1	31.8	34.8	-54.5
3	7-17-62	6.3	2.72	0.77	0.46	3.0	39.8	41.7	-34.5
4	7-17-62	6.4	2.68	0.80	0.46	3.0	52.5	55.0	-30.1
7	7-17-62	6.4	3.16	0.84	0.49	3.0	62.2	64.7	-21.6
10	7-17-62	6.4	3.17	0.73	0.49	3.0	68.2	70.0	-11.7
11	7-17-62	6.5	3.58	0.78	0.43	2.9	71.9	72.4	- 2.1
12	7-17-62	6.5	3.17	0.83	0.47	2.9	67.9	69.4	- 9.8
13	7-17-62	6.6	2.82	0.80	0.47	2.8	48.4	49.6	-18.7
14	7-17-62	6.6	2.99	0.80	0.58	2.8	69.4	70.5	- 6.2
15	7-17-62	6.7	3.71	0.80	0.44	2.8	73.5	72.0	10.9
16	7-17-62	6.7	3.40	0.81	0.46	2.8	54.7	53.6	17.5
17	7-17-62	6.8	2.77	0.83	0.50	2.7	37.1	36.5	16.1
30	7-17-62	6.8	3.65	0.84	0.47	2.7	14.5	13.9	46.2
18	7-17-62	6.9	3.15	0.83	0.41	2.7	35.9	34.5	38.5
19	7-17-62	6.9	3.07	0.80	0.45	2.7	71.5	69.4	16.7
20	7-17-62	6.9	3.02	0.83	0.48	2.7	77.7	75.0	14.9
21	7-17-62	7.0	2.90	0.83	0.49	2.6	70.4	67.8	22.2
22	7-17-62	7.1	3.16	0.84	0.48	2.5	59.5	57.4	27.8
23	7-17-62	7.2	3.35	0.83	0.46	2.5	57.0	54.9	30.6
24	7-17-62	7.2	3.74	0.83	0.45	2.5	47.9	45.6	41.3
26	7-17-62	7.3	2.71	0.83	0.53	2.4	39.0	36.6	53.3
27	7-17-62	7.4	3.71	0.83	0.45	2.4	26.1	23.7	66.3
28	7-17-62	7.7	3.36	0.88	0.39	2.2	40.8	38.7	51.1
29	7-17-62	7.7	2.54	0.83	0.47	2.2	30.7	29.3	47.7
1	7-17-62	8.5	2.66	0.81	0.47	1.7	26.6	28.3	-61.2
2	7-17-62	8.5	3.59	0.83	0.46	1.7	32.9	34.7	-54.8
3	7-17-62	8.6	2.85	0.84	0.43	1.7	40.6	41.7	-35.7
4	7-17-62	8.6	3.10	0.87	0.53	1.7	53.5	55.0	-30.7
7	7-17-62	8.7	3.24	0.91	0.50	1.6	63.2	64.6	-21.3
10	7-17-62	8.7	3.02	0.86	0.48	1.6	69.0	70.1	-12.4
11	7-17-62	8.7	3.50	0.84	0.46	1.6	72.2	72.5	- 2.9
12	7-17-62	8.8	3.09	0.88		1.6	68.5	69.2	- 9.3
13	7-17-62	8.9	2.76	0.84	0.51	1.5	48.9	49.5	-17.3
14	7-17-62	8.9	2.99	0.89	0.47	1.5	69.9	70.3	- 5.5
15	7-17-62	9.0	3.66	0.86	0.53	1.4	73.0	72.2	10.2
16	7-17-62	9.0	3.30	0.87	0.44	1.4	54.3	53.7	15.8
17	7-17-62	9.0	2.76	0.89	0.49	1.4	36.9	36.6	13.0
30	7-17-62	9.1	3.64	0.89	0.48	1.4	14.3	14.0	40.6
18	7-17-62	9.1	3.11	0.88	0.47	1.4	35.3	34.6	36.3
19	7-17-62	9.2	2.88	0.74	0.48	1.3	70.6	69.6	16.0
20	7-17-62	9.2	2.99	0.83	0.47	1.3	76.5	75.2	14.8
21	7-17-62	9.3	2.83	0.85	0.52	1.3	69.2	67.9	22.1
22	7-17-62	9.4	3.09	0.85	0.49	1.2	58.5	57.4	28.5
23	7-17-62	9.4	3.14	0.80	0.41	1.2	56.0	55.0	31.3
24	7-17-62	9.3	3.66	0.86	0.47	1.3	46.9	45.8	40.4
26	7-17-62	9.4	3.12	0.88	0.51	1.2	37.9	36.7	53.0
27	7-17-62	9.5	3.62	0.86	0.47	1.2	25.0	23.8	66.1
28	7-17-62	9.5	3.62	0.86	0.48	1.2	39.9	38.7	51.2
29	7-17-62	9.6	2.54	0.87	0.53	1.1	30.0	29.3	49.7
1	7-18-62	6.9	2.83	0.86	0.59	10.6	36.0	26.7	60.5
2	7-18-62	6.9	4.22	0.81	0.40	10.6	44.2	33.6	56.3
3	7-18-62	7.0	2.91	0.80	0.48	10.7	50.3	41.8	42.9
4	7-18-62	7.0	3.40	0.84	0.54	10.7	64.7	54.5	34.6
7	7-18-62	7.1	3.51	0.72	0.49	10.8	68.2	62.8	18.2
10	7-18-62	7.1	3.37	0.86	0.50	10.8	77.8	70.2	16.8

TABLE I (continued)

Object	Date	UT	V	B-V	U-B	g	A <sub>⊙</sub>	A <sub>⊕</sub>	α
11	7-18-62	7.2	3.75	0.80	0.47	10.8°	75.3°	73.5°	8.1°
12	7-18-62	7.2	3.43	0.91	0.55	10.8	67.4	67.5	5.2
13	7-18-62	7.2	3.04	0.81	0.49	10.8	48.2	47.8	7.1
14	7-18-62	7.3	3.29	0.89	0.52	10.9	66.9	68.7	1.5
15	7-18-62	7.3	4.28	0.82	0.43	10.9	68.0	74.0	- 5.3
16	7-18-62	7.4	3.69	0.85	0.50	10.9	52.5	55.4	- 5.3
17	7-18-62	7.4	3.06	0.87	0.54	10.9	38.3	38.1	6.2
30	7-18-62	7.4	4.08	0.85	0.47	10.9	15.5	15.5	6.0
18	7-18-62	7.5	3.56	0.84	0.48	11.0	32.6	36.4	-21.0
19	7-18-62	7.5	3.43	0.81	0.48	11.0	63.3	71.4	-11.5
20	7-18-62	7.6	3.39	0.85	0.49	11.0	65.5	76.4	-13.4
21	7-18-62	7.7	3.33	0.89	0.53	11.1	58.1	69.1	-20.7
22	7-18-62	7.7	3.61	0.84	0.48	11.1	47.3	57.8	-30.4
23	7-18-62	7.7	3.78	0.86	0.47	11.1	44.8	55.4	-33.0
24	7-18-62	9.7	4.21	0.83	0.48	12.2	38.0	47.7	-34.5
26	7-18-62	9.9	3.19	0.88	0.63	12.3	26.6	38.3	-50.0
27	7-18-62	9.9	3.56	0.82	0.46	12.3	13.2	25.3	-64.2
28	7-18-62	10.0	4.03	0.83	0.47	12.4	27.4	40.0	-49.8
29	7-18-62	10.0	3.09	0.87	0.52	12.4	19.2	29.1	-54.7
1	7-18-62	8.9	2.83	0.99	0.53	11.8	36.9	26.6	63.4
2	7-18-62	9.0	3.90	0.83	0.50	11.8	45.3	33.5	57.9
3	7-18-62	9.0	2.97	0.88	0.55	11.8	51.1	41.8	42.4
4	7-18-62	9.1	3.42	0.87	0.51	11.9	65.7	54.4	35.5
7	7-18-62	9.1	3.55	0.94	0.52	11.9	68.4	62.6	21.3
10	7-18-62	9.1	3.31	0.92	0.52	11.9	78.3	70.2	17.5
11	7-18-62	9.2	3.81	0.84	0.45	11.9	75.1	73.6	8.6
12	7-18-62	9.2	3.47	0.92	0.59	11.9	67.2	67.4	8.3
13	7-18-62	9.3	3.09	0.87	0.50	12.0	48.1	47.6	12.3
14	7-18-62	9.3	3.34	0.92	0.52	12.0	66.5	68.6	4.5
15	7-18-62	9.3	4.15	0.86	0.45	12.0	67.2	74.1	- 4.8
16	7-18-62	9.4	3.72	0.87	0.49	12.0	52.1	55.5	- 6.2
17	7-18-62	9.4	3.16	0.92	0.56	12.0	38.2	38.3	2.9
30	7-18-62	9.5	4.11	0.89	0.48	12.1	15.5	15.7	5.3
18	7-18-62	9.5	3.56	0.88	0.50	12.1	32.2	36.5	-22.8
19	7-18-62	9.6	3.43	0.83	0.52	12.2	62.4	71.6	-11.6
20	7-18-62	9.6	3.43	0.89	0.49	12.2	64.5	76.6	-13.3
21	7-18-62	9.6	3.31	0.94	0.54	12.2	57.1	69.2	-20.6
22	7-18-62	9.7	3.62	0.87	0.49	12.2	46.3	57.8	-30.2
23	7-18-62	9.8	3.40	0.87	0.53	12.3	43.8	55.4	-32.9
24	7-18-62	9.7	4.25	0.88	0.46	12.3	38.0	47.7	-34.5
26	7-18-62	9.9	3.35	0.93	0.56	12.3	26.6	38.3	-50.0
27	7-18-62	9.9	4.62	0.87	0.45	12.3	13.2	25.3	-64.2
28	7-18-62	10.0	4.06	0.82	0.47	12.4	27.7	40.0	-49.8
29	7-18-62	10.0	3.15	0.93	0.58	12.4	19.2	29.1	-54.7
1	7-19-62	8.5	2.95	0.87	0.53	25.0	46.9	24.7	63.2
2	7-19-62	8.5	4.46	0.82	0.90	25.0	57.2	32.2	57.8
3	7-19-62	8.4	3.09	0.83	0.54	24.9	59.2	41.7	42.4
4	7-19-62	8.4	3.62	0.85	0.51	24.9	76.2	53.6	35.3
7	7-19-62	8.3	3.88	0.86	0.51	24.9	68.7	60.6	21.1
10	7-19-62	8.3	3.51	0.90	0.50	24.9	77.4	70.0	17.4
11	7-19-62	8.3	4.11	0.82	0.48	24.9	69.0	74.3	8.5
12	7-19-62	8.2	3.78	0.83	0.52	24.8	61.7	65.5	8.1
13	7-19-62	8.1	3.27	0.87	0.53	24.8	45.7	45.9	12.0
14	7-19-62	8.1	3.67	0.89	0.54	24.8	59.8	66.9	4.3
15	7-19-62	8.0	4.47	0.85	0.46	24.7	57.8	76.0	- 4.9
16	7-19-62	8.0	4.03	0.88	0.51	24.7	46.5	57.3	- 6.3
17	7-19-62	8.0	3.42	0.91	0.56	24.7	36.5	39.7	2.9
30	7-19-62	7.9	4.48	0.86	0.49	24.7	14.9	17.2	- 5.1
18	7-19-62	7.9	4.04	0.87	0.53	24.7	27.1	38.4	-22.8
19	7-19-62	7.8	3.77	0.89	0.57	24.6	52.6	73.5	-11.0
20	7-19-62	7.8	3.74	0.85	0.52	24.6	53.2	77.9	-12.1
21	7-19-62	7.7	3.72	0.92	0.57	24.5	46.0	70.5	-19.5
22	7-19-62	7.6	4.14	0.85	0.44	24.5	35.6	58.3	-28.6
23	7-19-62	7.6	3.92	0.71	0.64	24.5	33.0	55.9	-31.3
24	7-19-62	7.7	4.74	0.85	0.49	24.5	28.6	49.6	-34.0
26	7-19-62	7.5	3.85	0.94	0.64	24.4	16.2	39.9	-49.0
27	7-19-62	7.5	3.46	0.76	0.34	24.4	2.5	26.7	-63.0
28	7-19-62	7.4	4.67	0.84	0.55	24.4	16.9	41.3	-48.7
1	7-19-62	10.8	2.99	0.91	0.50	26.3	47.8	24.5	63.4
2	7-19-62	10.8	4.42	0.82	0.40	26.3	58.3	32.1	57.9
3	7-19-62	10.8	3.19	0.90	0.59	26.3	59.9	41.6	42.4

TABLE I (continued)

Object	Date	UT	V	B-V	U-B	g	$A_{\odot}$	$A_{\oplus}$	$\alpha$
4	7-19-62	10.7	3.62	0.91	0.54	26.2°	77.1°	53.6°	35.5°
7	7-19-62	10.7	3.79	0.93	0.53	26.2	68.4	60.4	21.3
10	7-19-62	10.7	3.51	0.90	0.50	26.2	76.8	69.9	17.5
11	7-19-62	10.6	4.14	0.86	0.41	26.2	68.2	74.4	8.6
12	7-19-62	10.6	3.76	0.99	0.59	26.2	60.9	65.3	8.3
13	7-19-62	10.5	3.29	0.90	0.51	26.1	45.3	45.7	12.3
14	7-19-62	10.5	3.62	0.88	0.53	26.1	58.9	66.7	4.5
15	7-19-62	10.5	4.50	0.87	0.46	26.1	56.7	76.2	-4.8
16	7-19-62	10.4	4.05	0.88	0.52	26.1	45.8	57.4	-6.2
17	7-19-64	10.3	3.43	0.97	0.61	26.0	36.2	39.9	2.9
30	7-19-62	10.3	4.47	0.91	0.48	26.0	14.8	17.4	5.3
18	7-19-62	10.3	4.05	0.88	0.51	26.0	26.5	38.6	-22.8
19	7-19-62	10.2	3.69	0.96	0.57	26.0	51.4	73.7	-10.9
20	7-19-62	10.2	3.73	0.92	0.48	26.0	52.0	78.0	-12.0
21	7-19-62	10.1	3.62	0.97	0.58	25.9	44.8	70.7	-19.3
22	7-19-62	10.0	4.01	0.90	0.55	25.9	34.4	58.3	-28.4
23	7-19-62	10.0	3.86	0.81	0.51	25.9	31.8	56.0	-31.2
24	7-19-62	9.9	4.78	0.89	0.48	25.8			
26	7-19-62	9.9	4.26	0.86	0.56	25.8			
27	7-19-62	9.8	3.07	0.77	0.38	25.7	1.4	26.8	-62.9
28	7-19-62	9.8	4.83	0.74	0.60	25.7	15.7	41.4	-48.6
1	8-15-62	5.8	3.18	0.87	0.45	8.2			
2	8-15-62	5.9	4.43	0.78	0.26	8.1	25.9	34.0	-55.8
3	8-15-62	5.9	3.13	0.81	0.42	8.1	35.6	42.7	-42.7
4	8-15-62	6.0	3.56	0.84	0.38	8.1	47.2	55.2	-34.3
7	8-15-62	6.0	3.75	0.78	0.34	8.1	56.9	62.3	-17.2
10	8-15-62	6.1	3.45	0.73	0.42	8.0	63.8	71.1	-16.6
11	8-15-62	6.1	3.82	0.66	0.47	8.0	69.3	74.6	-8.0
12	8-15-62	6.2	3.49	0.91	0.53	8.0	64.2	66.7	-3.9
13	8-15-62	6.2	3.13	0.86	0.37	8.0	45.6	46.9	-5.0
14	8-15-62	6.3	3.29	0.88	0.42	7.9	66.4	67.8	-0.2
15	8-15-62	6.4	3.98	0.84	0.34	7.9			
16	8-15-62	6.5	3.66	0.85	0.40	7.8	56.4	56.3	4.3
17	8-15-62	6.6	3.12	0.92	0.44	7.7	37.8	39.1	-8.3
30	8-15-62	6.5	4.09	0.83	0.37	7.8	15.9	16.5	-12.3
18	8-15-62	6.6	3.46	0.86	0.41	7.7	38.8	37.2	18.5
19	8-15-62	6.8	3.25	0.93	0.48	7.6	75.3	71.9	11.4
20	8-15-62	6.8	3.36	0.84	0.32	7.6	83.6	76.1	13.7
21	8-15-62	6.9	3.20	0.87	0.46	7.6	76.3	68.8	21.0
22	8-15-62	6.9	3.49	0.88	0.39	7.6	64.0	57.0	31.3
23	8-15-62	7.0	3.58	0.88	0.39	7.5	61.7	54.6	34.0
24	8-15-62	6.9	4.03	0.86	0.35	7.6	53.1	47.9	33.5
26	8-15-62	7.0	3.03	0.93	0.54	7.5	45.0	38.1	49.7
27	8-15-62	7.1	4.03	0.86	0.36	7.5	32.1	24.9	64.2
28	8-15-62	7.1	3.70	0.88	0.40	7.5	46.9	39.6	50.1
29	8-15-62	7.2	2.79	0.89	0.43	7.4	34.1	28.2	56.8
1	8-15-62	8.4	3.14	0.67	0.56	18.1	37.0	19.6	69.9
2	8-15-62	8.5	4.27	0.86	0.35	18.1	46.1	28.2	61.6
3	8-15-62	8.5	2.98	0.84	0.49	18.0	52.8	40.8	40.8
4	8-15-62	8.6	3.47	0.89	0.52	18.0	67.0	50.9	37.4
7	8-15-62	8.6	3.60	0.90	0.50	17.9	67.2	55.0	29.6
10	8-15-62	8.7	3.37	0.91	0.41	17.9	80.0	68.2	19.5
11	8-15-62	8.7	3.73	0.88	0.36	17.9	76.3	74.9	10.1
12	8-15-62	8.7	3.49	0.98	0.44	17.9	65.5	60.3	17.4
13	8-15-62	8.8	3.03	0.89	0.47	17.8	46.5	40.9	27.0
14	8-15-62	8.8	3.23	0.93	0.40	17.8	64.9	61.9	13.6
15	8-15-62	8.9	4.04	0.89	0.42	17.8	67.7	81.0	-2.8
16	8-15-62	9.0	3.64	0.89	0.41	17.8	53.3	61.9	-8.1
17	8-15-62	9.0	3.12	0.97	0.43	6.4	38.1	39.3	-10.7
30	8-15-62	9.0	4.00	0.94	0.36	6.4	15.9	16.7	-18.5
18	8-15-62	9.1	3.46	0.94	0.37	6.3	38.5	37.4	15.9
19	8-15-62	9.1	3.49	0.70	0.35	6.3	74.9	72.1	10.7
20	8-15-62	9.2	3.26	0.90	0.37	6.3	82.4	76.3	13.5
21	8-15-62	9.3	3.21	0.92	0.41	6.2	75.1	69.0	20.7
22	8-15-62	9.3	3.43	0.88	0.35	6.2	62.9	57.1	31.5
23	8-15-62	9.3	3.21	0.90	0.36	6.2	60.6	54.7	34.2
24	8-15-62	9.2	3.99	0.90	0.35	6.3	52.3	48.1	32.5
26	8-15-62	9.4	3.01	1.00	0.43	6.2	43.9	38.3	49.1
27	8-15-62	9.5	3.96	0.90	0.34	6.1	30.9	25.1	63.8
28	8-15-62	9.5	3.68	0.97	0.40	6.1	45.7	39.7	49.7
29	8-15-62	9.6	2.78	0.93	0.40	6.1	33.2	28.2	57.4



TABLE I (continued)

Object	Date	UT	V	B-V	U-B	g	$A_{\odot}$	$A_{\oplus}$	$\alpha$
1	9-13-62	6.2	3.52	0.80	0.46	13.2°	14.1°	24.6°	-59.8°
2	9-13-62	6.3	4.63	0.77	0.39	13.1	20.2	32.9	-56.1
3	9-13-62	6.4	3.09	0.77	0.41	13.1	31.0	43.3	-44.6
4	9-13-62	6.4	3.55	0.87	0.52	13.1	41.7	54.8	-35.2
7	9-13-62	6.5	3.66	0.82	0.52	13.0	52.1	59.7	-14.8
10	9-13-62	6.6	3.38	0.87	0.48	12.9	58.8	71.5	-18.0
11	9-13-62	6.6	3.89	0.75	0.42	12.9	65.2	76.2	-10.1
12	9-13-62	6.7	3.49	0.96	0.57	12.9	60.6	63.9	-1.1
13	9-13-62	6.8	3.09	0.85	0.50	12.8	43.2	44.2	2.6
14	9-13-62	6.8	3.30	0.84	0.51	12.8	63.3	65.1	2.5
15	9-13-62	6.9	4.14	0.81	0.41	12.8	74.2	77.5	2.7
16	9-13-62	6.9	3.73	0.84	0.43	12.8	56.3	59.0	-1.3
17	9-13-62	7.0	3.21	0.86	0.49	12.7	37.2	41.7	-16.8
30	9-13-62	7.0	4.17	0.85	0.45	12.7	16.1	19.1	-30.6
18	9-13-62	7.0	3.55	0.86	0.48	12.7	40.3	40.0	8.1
19	9-13-62	7.2	3.32	1.06	0.56	12.6	76.6	74.5	8.7
20	9-13-62	7.2	3.34	0.83	0.42	12.6	88.9	77.1	12.9
21	9-13-62	7.3	3.31	0.87	0.48	12.5	82.0	69.8	19.9
22	9-13-62	7.5	3.49	0.86	0.47	12.4	68.4	56.8	32.1
23	9-13-62	7.5	3.30	0.91	0.56	12.4	66.4	54.5	34.7
24	9-13-62	7.4	4.09	0.85	0.44	12.5	57.3	50.3	28.5
26	9-13-62	7.6	3.01	0.92	0.58	12.4	50.4	39.9	46.5
27	9-13-62	7.6	4.02	0.84	0.45	12.4	37.8	26.4	61.7
28	9-13-62	7.6	3.66	0.82	0.45	12.4	52.6	40.8	48.3
29	9-13-62	7.7	2.80	1.00	0.55	12.3	38.0	27.3	59.6
1	9-13-62	8.5	3.49	0.90	0.49	11.9	15.1	24.4	-59.4
2	9-13-62	8.5	4.57	0.81	0.44	11.9	21.3	32.7	-56.0
3	9-13-62	8.5	3.18	0.85	0.56	11.9	32.0	43.3	-45.0
4	9-13-62	8.6	4.03	0.46	0.52	11.8	42.8	54.7	-35.3
7	9-13-62	8.6	3.53	0.90	0.54	11.8	53.0	59.4	-14.2
10	9-13-62	8.6	3.35	0.78	0.58	11.8	59.7	71.4	-18.3
11	9-13-62	8.7	3.90	0.82	0.40	11.8	66.1	76.3	-10.5
12	9-13-62	8.7	3.73	0.82	0.47	11.8	61.2	63.7	-0.4
13	9-13-62	8.7	3.31	0.88	0.52	11.8	43.5	44.0	3.4
14	9-13-62	8.8	3.34	0.88	0.53	11.7	63.8	65.0	3.1
15	9-13-62	8.9	4.13	0.82	0.44	11.6	74.7	77.7	2.2
16	9-13-62	8.9	3.70	0.84	0.45	11.6	56.5	59.2	-2.4
17	9-13-62	9.0	3.24	0.92	0.55	11.6	37.5	41.8	-18.4
30	9-13-62	8.9	4.17	0.88	0.48	11.6	16.2	19.2	-33.7
18	9-13-62	9.0	3.59	0.88	0.52	11.6	40.2	40.1	6.1
19	9-13-62	9.0	3.28	0.85	0.58	11.6	76.6	74.6	8.3
20	9-13-62	9.1	3.31	0.84	0.48	11.5	88.3	77.2	12.7
21	9-13-62	9.1	3.29	1.00	0.55	11.5	81.1	70.0	19.7
22	9-13-62	9.2	3.44	0.87	0.42	11.5	67.7	56.9	32.2
23	9-13-62	9.2	3.34	0.83	0.51	11.5	65.7	54.6	34.7
24	9-13-62	9.1	4.06	0.81	0.39	11.5	56.8	50.4	27.7
26	9-13-62	9.2	3.12	0.95	0.58	11.5	49.7	40.6	46.0
27	9-13-62	9.2	4.03	0.85	0.51	11.5	37.0	26.6	61.4
28	9-13-62	9.2	3.62	0.87	0.54	11.5	51.8	40.9	48.0
29	9-13-62	9.3	2.89	0.92	0.61	11.4	37.4	27.4	59.8
1	9-14-62	6.5	2.94	0.78	0.21	3.8	25.1	22.2	61.6
2	9-14-62	6.5	3.94	0.77	0.31	3.8	32.4	30.7	37.8
3	9-14-62	6.4	2.87	0.80	0.39	3.8	41.6	42.3	-10.3
4	9-14-62	6.4	3.26	0.82	0.39	3.8	53.6	53.1	9.0
7	9-14-62	6.3	3.36	0.81	0.34	3.8	60.9	57.4	31.2
10	9-14-62	6.3	3.11	0.79	0.35	3.8	69.9	70.2	0.4
11	9-14-62	6.3	3.67	0.78	0.29	3.8	74.1	76.0	-5.9
12	9-14-62	6.2	3.25	0.88	0.41	3.7	65.8	62.1	27.9
13	9-14-62	6.2	2.87	0.80	0.38	3.7	46.2	42.5	47.2
14	9-14-62	6.2	3.05	0.78	0.37	3.7	67.2	63.5	26.1
15	9-14-62	6.0	3.85	0.75	0.35	3.7	75.7	79.4	-10.6
16	9-14-62	6.0	3.47	0.78	0.33	3.7	57.0	60.6	-29.0
17	9-14-62	5.9	3.02	0.80	0.38	3.7	39.4	42.8	-44.9
30	9-14-62	5.9	3.85	0.80	0.33	3.7	16.8	20.4	-68.7
18	9-14-62	5.8	3.38	0.80	0.36	3.6	38.1	41.8	-48.2
19	9-14-62	5.8	3.10	0.78	0.36	3.6	73.4	76.7	-11.8
20	9-14-62	5.7	3.13	0.80	0.34	3.6	78.0	78.7	-0.1
21	9-14-62	5.7	3.03	0.88	0.41	3.6	70.8	71.6	-2.8
22	9-14-62	5.7	3.29	0.81	0.34	3.6	58.6	57.8	10.2
23	9-14-62	5.6	3.07	0.81	0.39	3.6	56.3	55.6	9.9
24	9-14-62	5.6	3.85	0.79	0.34	3.6	49.6	52.5	-31.0
26	9-14-62	5.6	2.85	0.85	0.45	3.6	40.1	41.9	-29.0

TABLE I (continued)

Object	Date	UT	V	B-V	U-B	g	$A_{\odot}$	$A_{\oplus}$	$\alpha$
27	9-14-62	5.4	3.86	0.79	0.33	3.6°	27.0°	28.4°	-34.8°
28	9-14-62	5.4	3.55	0.81	0.34	3.6	41.6	42.6	-14.4
29	9-14-62	5.4	2.68	0.79	0.32	3.6	29.6	27.9	42.8
1	9-14-62	9.8	2.82	0.88	0.39	5.0	26.5	21.9	66.9
2	9-14-62	9.8	4.03	0.78	0.30	5.0	34.1	30.4	52.0
3	9-14-62	9.7	2.84	0.77	0.38	4.9	43.0	42.2	13.1
4	9-14-62	9.6	3.29	0.84	0.41	4.9	55.3	52.8	22.7
7	9-14-62	9.6	3.46	0.87	0.35	4.9	61.9	57.1	32.9
10	9-14-62	9.5	3.22	0.85	0.36	4.8	71.3	69.9	8.1
11	9-14-62	9.5	3.60	0.78	0.37	4.8	75.0	75.9	-0.5
12	9-14-62	9.4	3.46	0.90	0.33	4.8	66.2	61.9	26.0
13	9-14-62	9.4	2.92	0.82	0.36	4.8	46.4	42.3	43.7
14	9-14-62	9.4	3.15	0.88	0.41	4.8	67.3	63.3	23.3
15	9-14-62	9.3	3.92	0.82	0.35	4.7	75.2	79.6	-9.4
16	9-14-62	9.1	3.47	0.78	0.33	4.7	56.8	60.8	-25.1
17	9-14-62	9.0	2.97	0.82	0.37	4.6	39.5	42.9	-37.3
30	9-14-62	9.1	3.84	0.84	0.38	4.7	17.0	20.5	-63.8
18	9-14-62	9.0	3.39	0.87	0.38	4.6	37.7	42.0	-45.9
19	9-14-62	9.0	3.15	0.74	0.44	4.6	72.4	77.0	-13.0
20	9-14-62	8.9	3.16	0.84	0.37	4.6	76.5	78.9	-4.3
21	9-14-62	8.9	3.34	0.84	0.38	4.6	69.1	71.9	-9.6
22	9-14-62	8.9	3.33	0.82	0.36	4.6	57.1	57.9	-3.9
23	9-14-62	8.8	3.12	0.86	0.40	4.5	54.8	55.7	-5.8
24	9-14-62	8.8	3.87	0.81	0.36	4.5	48.4	52.8	-36.3
26	9-14-62	8.7	3.05	0.86	0.40	4.5	38.6	42.3	-41.2
27	9-14-62	8.7	3.92	0.80	0.34	4.5	25.4	28.7	-53.1
28	9-14-62	8.7	3.64	0.84	0.33	4.5	40.0	42.7	-33.8
29	9-14-62	8.7	2.71	0.87	0.37	4.5	28.3	28.0	-8.7
1	9-15-62	6.8	2.89	0.86	0.47	16.4	35.7	19.8	69.7
2	9-15-62	6.8	4.25	0.76	0.26	16.4	49.7	28.5	61.3
3	9-15-62	6.7	2.99	0.78	0.55	16.3	51.6	41.0	40.0
4	9-15-62	6.7	3.48	0.89	0.46	16.3	65.6	51.1	36.9
7	9-15-62	6.6	3.51	0.96	0.46	16.3	66.9	55.2	29.7
10	9-15-62	6.6	3.39	0.93	0.49	16.3	79.3	68.4	19.0
11	9-15-62	6.6	3.95	0.86	0.38	16.3	76.7	75.0	9.6
12	9-15-62	6.5	3.60	0.94	0.56	16.2	65.9	60.4	17.7
13	9-15-62	6.5	3.06	0.83	0.43	16.2	46.7	41.1	27.8
14	9-15-62	6.5	3.32	0.88	0.45	16.2	65.4	62.1	13.9
15	9-15-62	6.3	4.21	0.82	0.38	16.1	68.9	80.9	
16	9-15-62	6.1	3.83	0.81	0.41	16.0	53.9	61.8	
17	9-15-62	6.1	3.39	0.91	0.48	16.0	39.7	43.6	-7.1
30	9-15-62	6.1	4.25	0.83	0.38	16.0	17.0	21.4	-29.8
18	9-15-62	6.0	3.73	0.83	0.40	15.9	34.0	43.4	-28.2
19	9-15-62	6.0	3.49	0.79	0.49	15.9	64.3	78.9	-9.1
20	9-15-62	5.9	3.44	0.78	0.45	15.9	65.8	80.4	-7.6
21	9-15-62	5.9	3.33	0.95	0.54	15.9	58.5	73.6	-14.9
22	9-15-62	5.8	3.67	0.86	0.43	15.8	47.2	59.0	-21.2
23	9-15-62	5.8	3.46	0.78	0.47	15.8	44.7	56.9	-24.1
24	9-15-62	5.7	4.35	0.81	0.34	15.7	40.0	54.8	-33.0
26	9-15-62	5.7	3.44	0.95	0.57	15.7	28.5	44.3	-45.7
27	9-15-62	5.7	4.76	0.88	0.33	15.7	15.0	30.7	-59.2
28	9-15-62	5.7	3.21	0.88	0.42	15.7	29.4	44.8	-44.3
29	9-15-62	5.6	3.20	0.87	0.50	15.7	19.7	28.7	-44.2
1	9-15-62	9.8	2.91	0.88	0.56	18.1	37.0	19.6	69.9
2	9-15-62	9.7	4.29	0.78	0.35	18.1	46.1	28.2	61.6
3	9-15-62	9.6	3.16	0.66	0.49	18.0	52.8	40.8	40.8
4	9-15-62	9.6	3.50	0.86	0.52	18.0	67.0	50.9	37.4
7	9-15-62	9.5	3.65	0.84	0.50	17.9	67.2	55.0	29.6
10	9-15-62	9.5	3.46	0.85	0.41	17.9	80.0	68.2	19.5
11	9-15-62	9.5	4.08	0.82	0.36	17.9	76.3	74.9	10.1
12	9-15-62	9.4	3.68	0.82	0.44	17.9	65.5	60.3	17.4
13	9-15-62	9.3	3.12	0.85	0.47	17.8	46.5	40.9	27.0
14	9-15-62	9.3	3.43	0.90	0.40	17.8	64.9	61.9	13.6
15	9-15-62	9.3	4.25	0.82	0.42	17.8	67.7	81.0	-2.8
16	9-15-62	9.2	3.89	0.85	0.41	17.8	53.3	61.9	-8.1
17	9-15-62	9.0	3.26	0.86	0.42	17.6	39.6	43.7	-5.4
30	9-15-62	9.0	4.24	0.84	0.44	17.6	17.0	21.5	-26.9
18	9-15-62	8.9	3.80	0.91	0.56	17.6	33.4	43.5	-26.9
19	9-15-62	8.9	3.56	0.76	0.38	17.6	63.0	79.1	-8.6
20	9-15-62	8.9	3.47	0.85	0.43	17.6	64.3	80.6	-7.5
21	9-15-62	8.8	3.24	0.85	0.95	17.5	57.1	73.8	-14.8

TABLE I (continued)

Object	Date	UT	V	B-V	U-B	g	A <sub>⊙</sub>	A <sub>⊕</sub>	α
22	9-15-62	8.8	3.74	0.84	0.41	17.5°	45.8°	59.1°	-21.5°
23	9-15-62	8.7	3.47	0.84	0.44	17.5	43.3	57.0	-24.4
24	9-15-62	8.6	4.41	0.83	0.39	17.4	38.8	55.1	-32.4
26	9-15-62	8.6	3.40	0.96	0.51	17.4	27.1	44.6	-45.4
27	9-15-62	8.5	4.81	0.91	0.87	17.4	13.7	31.0	-59.0
28	9-15-62	8.4	4.04	0.85	0.45	17.3	28.1	45.0	-44.2
29	9-15-62	8.3	3.25	0.78	0.46	17.2	18.6	28.9	-45.0
1									
2	12-9-62	7.6	3.02	0.87	0.37	28.4	0.5	27.8	-61.1
3	12-9-62	7.7	3.80	0.83	0.52	28.3	13.4	40.7	-48.0
4	12-9-62	7.8	4.14	0.95	0.41	28.2	22.3	50.5	-39.4
7	12-9-62	7.8	4.01	0.95	0.49	28.2	35.3	54.5	-19.7
10	12-9-62	7.9	3.90	0.91	0.44	28.2	39.7	67.9	-22.1
11	12-9-62	7.9	4.25	0.90	0.48	28.2	47.4	74.8	-14.1
12	12-9-62	8.0	3.83	0.93	0.44	28.1	46.2	59.7	-5.5
13	12-9-62	8.1	3.39	0.88	0.46	28.1	33.9	40.4	-2.7
14	12-9-62	8.1	3.65	0.93	0.53	28.1	49.6	61.4	-1.8
15	12-9-62	8.2	3.47	0.88	0.40	28.0	59.6	81.5	-1.3
16	12-9-62	8.2	4.07	0.90	0.45	28.0	48.2	62.4	-4.9
17	12-9-62	8.4	3.62	0.91	0.47	27.9	30.1	44.0	-19.2
30	12-9-62	8.3	4.56	0.93	0.45	28.0	13.4	21.9	-29.3
18	12-9-62	8.4	3.82	0.93	0.44	27.9	39.7	44.1	4.2
19	12-9-62	8.5	3.48	0.90	0.49	27.9	65.2	79.8	4.7
20	12-9-62	8.5	3.60	0.92	0.46	27.9	70.8	80.8	8.8
21	12-9-62	8.5	3.43	0.81	0.44	27.9	78.0	74.2	15.8
22	12-9-62	8.6	3.77	0.92	0.45	27.8	77.4	59.3	28.3
23	12-9-62	8.6	3.46	0.92	0.47	27.8	77.9	57.2	30.8
24	12-9-62	8.7	4.43	0.89	0.44	27.7	64.5	55.8	24.0
26	12-9-62	8.7	3.05	0.89	0.45	27.7	67.3	45.2	41.8
27	12-9-62	8.8	4.20	0.89	0.47	27.7	56.6	31.6	56.8
28	12-9-62	8.8	3.97	0.92	0.41	27.7	72.1	45.5	43.9
29	12-9-62	8.9	2.90	0.89	0.44	27.6	50.6	29.0	56.8
1									
2	12-10-62	5.0	4.57	0.84	0.47	16.5	6.1	18.2	-65.5
3	12-10-62	5.1	4.82	0.85	0.42	16.4	11.4	26.6	-61.4
4	12-10-62	5.2	3.11	0.84	0.50	16.3	23.2	39.3	-50.2
7	12-10-62	5.2	3.52	0.86	0.50	16.3	33.0	49.2	-40.4
10	12-10-62	5.2	3.59	0.91	0.50	16.3	44.8	54.0	-17.5
11	12-10-62	5.3	3.40	0.83	0.46	16.3	50.3	66.5	-23.4
12	12-10-62	5.3	3.73	0.92	0.48	16.3	57.4	73.4	-16.0
13	12-10-62	7.9	3.51	0.84	0.43	14.9	55.6	59.9	-2.8
14	12-10-62	7.9	3.16	0.85	0.45	14.9	40.1	40.8	4.4
15	12-10-62	7.8	3.29	0.87	0.49	14.9	58.6	61.7	0.6
16	12-10-62	7.8	4.10	0.87	0.42	14.9	69.4	80.7	-3.9
17	12-10-62	7.7	3.68	0.86	0.46	15.6	54.0	61.6	-10.2
30	12-10-62	7.7	3.20	0.88	0.49	15.0	34.8	43.6	-26.7
18	12-10-62	7.7	4.18	0.88	0.47	15.0	15.2	21.1	-42.7
19	12-10-62	7.6	3.50	0.89	0.46	15.0	40.7	43.7	-4.8
20	12-10-62	7.5	3.15	0.89	0.47	15.1	73.7	79.9	2.0
21	12-10-62	5.8	3.27	0.88	0.48	16.0	81.5	82.2	7.6
22	12-10-62	5.8	3.10	0.87	0.54	16.0	87.9	75.5	14.4
23	12-10-62	5.8	3.40	0.83	0.43	16.0	74.9	60.7	27.9
24	12-10-62	5.7	3.22	0.87	0.46	16.1	73.5	58.6	30.4
26	12-10-62	5.7	3.92	0.87	0.45	16.1	61.9	56.3	19.8
27	12-10-62	5.6	2.78	0.91	0.51	16.1	58.7	46.2	38.7
28	12-10-62	5.5	4.02	0.86	0.44	16.2	46.7	32.7	54.3
29	12-10-62	5.5	3.63	0.89	0.54	16.2	61.8	46.8	41.8
30	12-10-62	5.5	2.67	0.92	0.51	16.2	44.5	30.3	56.9
1									
2	12-10-62	8.8	4.95	0.78	0.44	14.4	7.8	18.1	-65.0
3	12-10-62	8.7	4.81	0.84	0.39	14.4	13.2	26.4	-61.3
4	12-10-62	8.7	3.16	0.82	0.51	14.4	24.8	39.0	-50.6
7	12-10-62	8.7	3.58	0.86	0.43	14.4	34.8	49.0	-40.4
10	12-10-62	8.6	3.75	0.83	0.42	14.5	46.3	54.0	-16.7
11	12-10-62	8.6	3.40	0.92	0.51	14.5	51.9	66.3	-23.6
12	12-10-62	8.6	3.72	0.89	0.49	14.5	58.9	73.2	-16.3
13	12-10-62	8.5	3.46	0.94	0.48	14.5	55.8	59.9	-2.7
14	12-10-62	8.5	3.01	0.85	0.45	14.5	40.2	40.8	4.7
15	12-10-62	8.5	3.23	0.89	0.49	14.5	58.9	61.8	0.8
16	12-10-62	8.4	4.12	0.86	0.42	14.6	69.6	80.6	-4.0
17	12-10-62	8.4	3.64	0.88	0.47	14.6	54.1	61.6	-10.4
30	12-10-62	8.3	3.33	0.90	0.51	14.6	34.9	43.0	-27.0
30	12-10-62	8.4	4.10	0.84	0.37	14.6	15.2	21.1	-43.2

TABLE I (continued)

Object	Date	UT	V	B-V	U-B	g	A <sub>⊙</sub>	A <sub>⊕</sub>	α
18	12-10-62	8.3	3.50	0.88	0.46	14.6°	40.7°	43.7°	- 5.2°
19	12-10-62	8.3	3.21	0.89	0.47	14.6	73.9	79.9	1.9
20	12-10-62	8.2	3.28	0.87	0.43	14.7	82.7	82.4	7.5
21	12-10-62	8.2	3.12	0.89	0.50	14.7	88.2	75.7	14.2
22	12-10-62	8.2	3.46	0.88	0.47	14.7	74.2	60.8	27.9
23	12-10-62	8.2	3.33	0.88	0.43	14.7	72.7	58.8	30.4
24	12-10-62	8.1	4.03	0.89	0.42	14.8	61.4	56.4	19.0
26	12-10-62	8.1	2.84	0.91	0.47	14.8	67.6	46.3	38.2
27	12-10-62	8.1	3.99	0.87	0.43	14.8	45.4	32.8	53.8
28	12-10-62	8.0	3.69	0.92	0.47	14.8	60.6	46.9	41.5
29	12-10-62	8.0	2.69	0.87	0.46	14.8	43.6	30.5	57.0
1	1- 9-63	6.2	3.30	0.85	0.43	9.0	11.2	18.2	-66.8
2	1- 9-62	6.2	4.30	0.82	0.37	9.0	16.7	25.3	-63.5
3	1- 9-62	6.3	2.98	0.83	0.45	9.0	27.6	36.2	-52.7
4	1- 9-62	6.4	3.34	0.81	0.43	8.9	38.2	47.1	-42.8
7	1- 9-62	6.4	3.36	0.83	0.43	8.9	49.7	55.2	-21.0
10	1- 9-62	6.5	3.17	0.86	0.44	8.8	55.2	64.0	-25.9
11	1- 9-63	6.6	3.52	0.83	0.42	8.8	61.9	70.1	-18.3
12	1- 9-63	6.6	3.26	0.90	0.49	8.8	59.0	62.2	- 7.2
13	1- 9-63	6.7	2.85	0.79	0.42	8.7	42.5	43.5	- 2.5
14	1- 9-63	6.7	3.05	0.83	0.41	8.7	61.9	64.4	- 3.7
15	1- 9-63	6.8	3.84	0.83	0.41	8.7	71.7	77.2	- 5.6
16	1- 9-63	6.8	3.41	0.83	0.43	8.7	54.7	58.3	-10.7
17	1- 9-63	6.8	2.88	0.84	0.43	8.7	35.5	39.6	-27.0
30	1- 9-63	6.9	3.81	0.89	0.43	8.6	15.0	17.7	-43.1
18	1- 9-63	6.9	3.22	0.86	0.43	8.6	39.9	40.8	- 3.1
19	1- 9-63	8.6	3.03	0.85	0.45	7.8	75.3	77.3	0.2
20	1- 9-63	8.7	2.98	0.87	0.42	7.7	87.2	84.8	5.1
21	1- 9-63	8.7	2.85	0.82	0.43	7.7	84.4	77.5	12.0
22	1- 9-63	8.7	3.05	0.89	0.44	7.7	71.2	64.0	24.9
23	1- 9-63	8.7	3.14	0.87	0.27	7.7	69.2	61.8	27.4
24	1- 9-63	8.8	3.72	0.87	0.41	7.7	58.3	55.1	18.8
26	1- 9-63	8.9	2.58	0.83	0.46	7.6	52.7	46.7	37.6
27	1- 9-63	8.9	3.67	0.86	0.41	7.6	40.3	33.6	53.2
28	1- 9-63	8.9	3.35	0.84	0.42	7.6	55.3	48.3	40.0
29	1- 9-63	8.9	2.44	0.83	0.41	7.6	40.5	33.9	52.9
1	1- 9-63	9.3	3.08	0.82	0.39	7.4	12.6	18.3	-66.4
2	1- 9-63	9.3	4.10	0.83	0.39	7.4	18.3	25.3	-63.4
3	1- 9-63	9.3	2.77	0.80	0.40	7.4	28.9	36.1	-53.0
4	1- 9-63	9.4	3.22	0.86	0.42	7.3	39.7	47.0	-42.9
7	1- 9-63	9.4	3.16	0.87	0.45	7.3	51.0	55.3	-20.4
10	1- 9-63	9.4	3.06	0.87	0.45	7.3	56.6	63.9	-26.0
11	1- 9-63	9.5	3.41	0.85	0.42	7.3	63.1	70.0	-18.5
12	1- 9-63	9.5	3.13	0.85	0.41	7.3	59.9	62.4	- 6.7
13	1- 9-63	9.6	2.73	0.84	0.42	7.2	43.1	43.7	- 1.2
14	1- 9-63	9.6	2.92	0.84	0.44	7.2	62.8	64.5	- 3.1
15	1- 9-63	9.6	3.75	0.85	0.40	7.2	72.5	77.0	- 6.0
16	1- 9-63	9.6	3.33	0.83	0.40	7.2	55.1	58.1	-11.6
17	1- 9-63	9.7	2.81	0.86	0.43	7.2	35.9	39.4	-28.4
30	1- 9-63	9.7	3.71	0.88	0.44	7.2	15.1	17.5	-45.5
18	1- 9-63	9.7	3.22	0.86	0.43	7.2	39.8	40.7	- 4.8
19	1- 9-63	9.8	2.93	0.86	0.44	7.1	75.4	77.3	0.02
20	1- 9-63	9.8	3.01	0.86	0.43	7.1	87.6	84.8	5.1
21	1- 9-63	9.8	2.82	0.82	0.40	7.1	83.9	77.3	11.9
22	1- 9-63	9.8	3.25	0.86	0.42	7.1	70.7	64.0	24.9
23	1- 9-63	9.9	3.07	0.85	0.40	7.1	68.7	61.9	27.4
24	1- 9-63	9.9	3.74	0.85	0.41	7.1	58.0	55.1	18.5
26	1- 9-63	10.0	2.53	0.86	0.47	7.0	52.2	46.7	37.4
27	1- 9-63	10.0	3.68	0.85	0.41	7.0	39.7	33.6	53.0
28	1- 9-63	10.0	3.41	0.87	0.43	7.0	54.8	48.3	39.9
29	1- 9-63	10.1	2.45	0.83	0.41	7.0	40.1	33.9	53.0

and

$$\Delta V = 0.0262\Delta g - 0.00220\Delta\alpha, \tag{2}$$

where the above angles are expressed in degrees. The average absolute value of the deviation of the observed  $\Delta V/\Delta g$  from that predicted by *either* formula was evaluated at 0.0129. Now it may be readily shown,

using the law of cosines and the law of sines of spherical trigonometry, that

$$\cos\alpha = \frac{\pm\sin A_{\oplus}}{\{1 - \cos^2 A_{\oplus} + [(\sin A_{\odot} - \cos g \sin A_{\oplus})/\sin g]^2\}^{\frac{1}{2}}}. \tag{3}$$

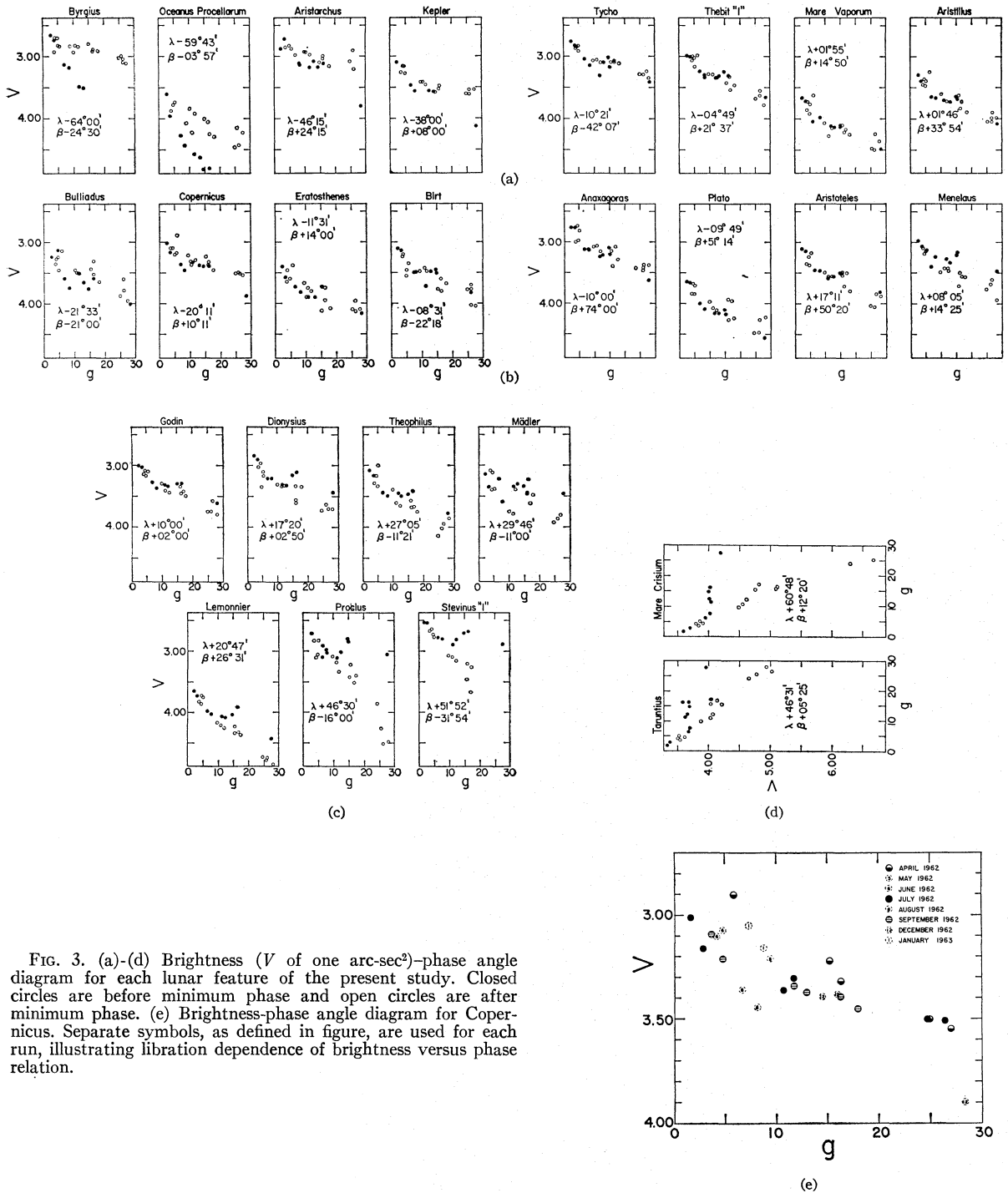


FIG. 3. (a)-(d) Brightness ( $V$  of one arc-sec<sup>2</sup>)-phase angle diagram for each lunar feature of the present study. Closed circles are before minimum phase and open circles are after minimum phase. (e) Brightness-phase angle diagram for Copernicus. Separate symbols, as defined in figure, are used for each run, illustrating libration dependence of brightness versus phase relation.

Differentiating this expression and substituting *rough* estimates of the average values of the parameters involved ( $g=15^\circ$ ,  $A_\oplus=60^\circ$ ,  $A_\odot=45^\circ$ ,  $|\alpha|=23^\circ$ ) one obtains:

$$d\alpha = -1.0dA_\oplus + 0.72dA_\odot + 13.3dg. \quad (4)$$

Combining (4) and (2) one predicts coefficients of  $\Delta A_\odot$

and  $\Delta A_\oplus$  whose algebraic signs and relative proportion are in substantial agreement with Eq. (1).

Accordingly, we conclude that the moon's photometric function, over our observational range, can be well approximated by a  $(g, \alpha)$ -dependent model. This conclusion had been previously reached by Fessenkov (1928) and Minnaert (1961) from the measurement of

TABLE II. List of lunar objects and correlated data.

Object	Strati- graphy	Ph.fn. resid.	$V(5^\circ)$	$B-V$
1 Byrgius	C	-.02205	2.82	.865
2 Oceanus Procellarum	P	.00530	3.86	.822
3 Aristarchus	C	.00270	2.84	.820
4 Kepler	C	-.00721	3.28	.866
7 Bulliadus	CE	-.01053	3.30	.871
10 Copernicus	C	.00193	3.18	.862
11 Eratosthenes	E	.00101	3.58	.849
12 Birt	C	.00014	3.40	.889
13 Tycho	C	-.00394	2.88	.850
14 Thebit "1"	C	-.00084	3.10	.874
15 Mare Vaporum	P	-.00001	3.86	.840
16 Aristillus	C	.00012	3.44	.856
17 Anaxagoras	C	.00574	2.90	.889
30 Plato	P	.00571	3.78	.873
18 Aristoteles	CE	.00477	3.30	.884
19 Menelaus	C	-.00559	3.21	.846
20 Godin	C	-.00195	3.21	.861
21 Dionysius	C	-.00487	3.11	.878
22 Theophilus	CE	-.00004	3.25	.865
23 Madler	CE	-.00941	3.24	.862
24 Le Monnier	P	.00693	3.88	.854
26 Proclus	C	.00367	2.88	.919
27 Mare Crisium	P	.01650	3.91	.843
28 Taruntius	CE	.01156	3.55	.870
29 Stevinius "1"	C	-.00218	2.78	.874

isophotes on a given photographic plate together with a number of normalization assumptions. The present conclusion is important for having been reached only by measurement of *brightness changes* and for its application over a phase range nearer to full moon than is possible with the Fessenkov-Minnaert technique.

#### B. Stratigraphy versus Residual from the Photometric Function

The placing of the objects of the present study in a stratigraphic sequence (Shoemaker and Hackman 1962)

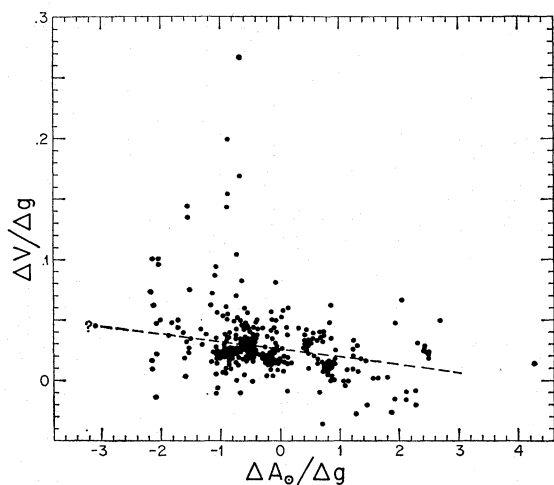


FIG. 4. Diagram of change in  $V$  magnitude plotted versus change in sun altitude for a given change in phase angle. Each point represents a pair of observations.

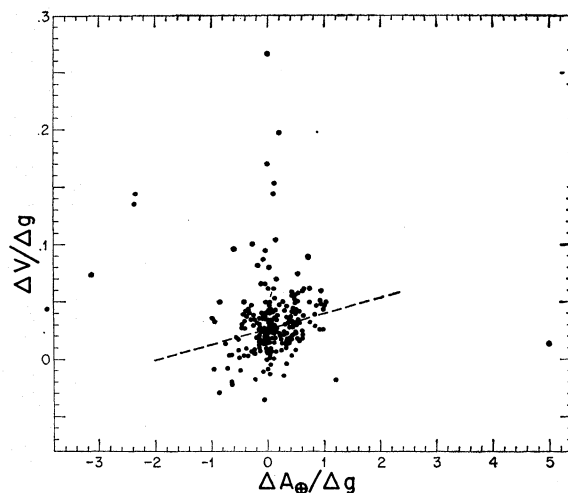


FIG. 5. Diagram of change in  $V$  magnitude plotted against change in earth altitude, both divided by corresponding change in phase angle.

has kindly been provided by Shoemaker (private communication). The sequence runs: (1) Copernican (C), (2) Copernican-Eratosthenian (CE), (3) Eratosthenian (E), and (4) Procellarian (P). This classification is shown in column 2 of Table II. Column 3 shows the average residual of the observed  $\Delta V/\Delta g$  from that predicted by Eq. (2), neglecting observations rejected in the least-squares solution, for the lunar feature of column 1. Figure 7 shows stratigraphy versus photometric function residual. There is a small trend indicating that Copernican reorientational brightness variations are less than average while Procellarian brightness variations are greater than average. The extent of agreement between the photometric functions of the various lunar strata is striking, however.

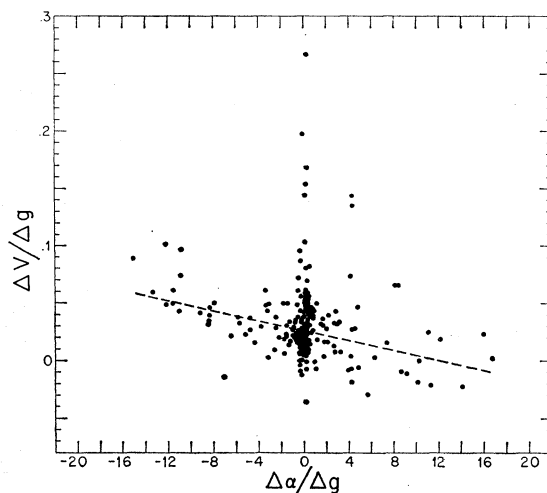
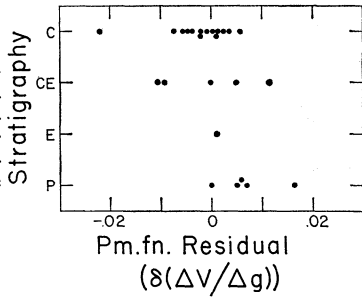


FIG. 6. As in Figs. 4 and 5 but replacing, respectively, sun altitude and earth altitude by brightness-longitude.

FIG. 7. Stratigraphy versus residual from photometric function. Residuals are averaged for each lunar feature, indicated by number, of the study.



C. Nominal Brightness at 5° Phase versus Stratigraphy

The value of  $V$  at a phase angle of  $5^\circ$  has been read from the plots of Fig. 3, averaging the waxing and waning portions. This is a parameter that can be read with far greater precision than would be involved in the extrapolation of  $V$  to  $0^\circ$  as is evident from Fig. 3. The result is shown in column 4 of Table II. A plot of  $V(5^\circ)$  versus stratigraphy is shown in Fig. 8. There is a clear trend of increasing brightness from Procellarian to Copernican. The correlation between  $V(5^\circ)$  and photometric function residual, suggested by these graphs, does exist, as may be verified by examining the data in Table II.

D. Nominal Brightness at 5° Phase versus Maximum Slope

Pohn (1963) has obtained the values of the maximum slope of the terrain in the vicinity of the features of the present study. His values may be underestimates, but by no more than  $12^\circ$ . These slopes are presenting the light examined only for craters smaller than the focal plane diaphragm. In others, like Tycho and Copernicus, they are the slopes of crater walls surrounding the crater floor which is actually being observed. The slopes are thus of less importance through a change of  $\alpha$  in the photometric function than as possible indicatrices of some geological delineation for the region of some more obscure origin. In Fig. 9,  $V(5^\circ)$  is plotted against maximum slope. There appears to be a trend of increasing slope with increasing brightness for objects fainter than  $V=3$ , and a much shallower trend in the reverse direction for brighter objects.

FIG. 8. Nominal brightness at 5° phase, waxing and waning averaged, as expressed by  $V$  of 1 arc-sec<sup>2</sup>, versus stratigraphy.

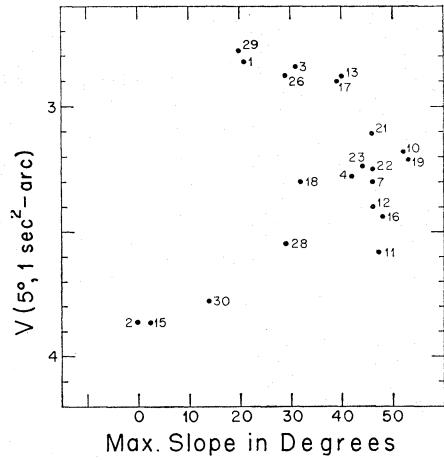
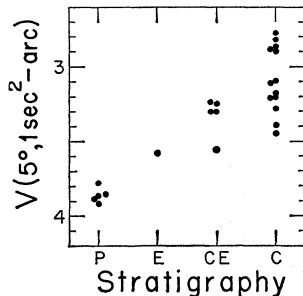


FIG. 9.  $V$  at 5° phase, waxing and waning, and libration effects averaged, versus maximum slope in or near region observed.

E. Color-Magnitude Diagram

Inasmuch as no clear-cut variation of color takes place with phase change, all the  $B-V$  observations have been averaged for each lunar feature and appear in column 5 of Table II.  $V$  at  $5^\circ$  phase is plotted against  $B-V$  in Fig. 10. There is a small trend from blue to red with increasing brightness for objects fainter than  $V=3$ . Above this there is a wide spread in color index over a small range in brightness with no apparent correlation. In both Figs. 9 and 10 the sequences brighter than  $V=3$  exhibit detached behavior compared to the remainders of the diagrams. Whether  $V=3$  is a real bifurcation cannot be decided due to a paucity of points. The same objects lie in this upper branch in both diagrams, but within the branch the correlation of  $B-V$  and maximum slope is poor. This correlation is better for the

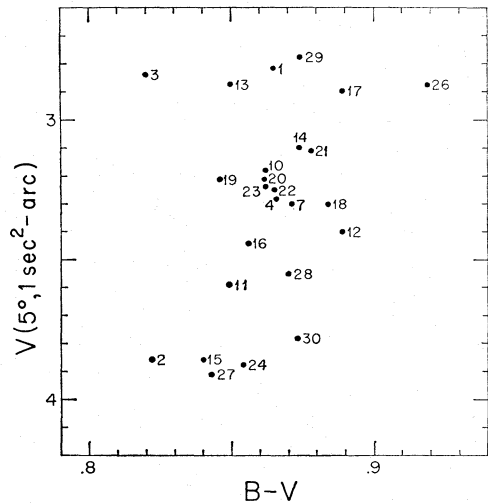


FIG. 10. Color-magnitude diagram for lunar features observed.  $V$  at 5° phase is plotted against  $B-V$  averaged for all observations of each object.

remainders of the two diagrams. This may be found examining Table II.

#### IV. DISCUSSION

These data cannot be the proof of any complete theory of evolution of the moon's surface. But we may assemble the following speculations into a fairly consistent hypothesis as far as the present study is concerned.

The photometric function of the moon provides for a great deal of backscatter which is consistent with a highly cavitateous surface, the exact detail of which we cannot specify, since a statistical model has yet to be proposed which exactly reproduces the moon's photometric function. Considering the sequence C → P as a progression in age, Fig. 7 implies that younger features on the moon remain more uniformly bright as orientation angles change, when compared to older features. Thus, as poorer backscatterers, they suggest an increase of cavitateousness with age. This could conceivably arise from micrometeorite erosion, providing resedimentation entailed something like vacuum welding and net matter loss was not too high. It might also arise from sputtering under extreme solar corpuscular radiation. Figure 8 implies lunar material darkens with age which is a reasonable consequence of accumulated radiation damage (Kohn and Benjamin 1961).

Interpretation of Figs. 9 and 10 is even more conjectural. Let us suppose that when a region of the moon is freshly exposed it possesses one of a variety of native colors—even though from a rather narrow range by earth standards, which may or may not be due to observational resolution. Let these features also be characterized by a range of slopes depending on the amount of light rubble present. One might conceive of slopes steepening in many cases as fine rubble is burnished away by micrometeorite flux. Exposing the underlying, coarser, post-disturbed surface the evolution of heterogeneity in color into homogeneity, corresponding to the average of colors of objects in the youngest phase, suggests intermixing of the materials of young objects. It might thus be suggested that the

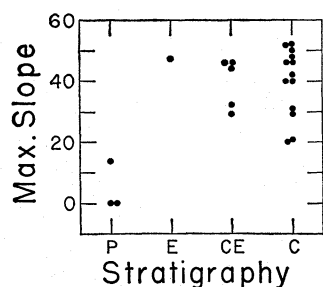


FIG. 11. Maximum slope in the vicinity of observed region versus stratigraphic class.

homogeneous grouping is constituted by objects old enough to have received a large fraction of ground cover made up of ejecta from many other parts of the moon. What is the nature of the equilibrium between this effect and the burnishing which removes primary rubble and ought to have a similar effect on this ejecta blanket? The answer might be found in the relative particle size, *shape*, and depth of cover for these two classes of debris.

Finally, as we tend toward the oldest objects at the faint ends of Figs. 9 and 10, we would find that the bluing effect was yielded by long exposure to radiation. In addition the older objects have shallower slopes because of the smoothing of long-term erosion and sedimentation *in situ* by larger, slower, more infrequent particles provided by secondary and higher impacts; and of course at the oldest extreme of this study we have the near flat surfaces of "flows" solidified under gravitational equilibrium—the maria.

It is interesting to note that if the sequences in Figs. 9 and 10 are, in fact, evolutionary it must be predicted that, on the average, the steepest slopes should occur for objects of intermediate age, rather than at either extreme. Figure 11 shows a plot of maximum slope versus stratigraphy in which this conclusion appears to be supported.

More satisfactory explanations may certainly exist, and a great wealth of further data with which to better define the last five diagrams of this study is needed. To the latter end the authors are presently in process of compiling a photometric atlas of the moon.

It is a pleasure to acknowledge stimulating discussions with Dr. B. C. Murray and Dr. E. M. Shoemaker. This study has been supported in part by the National Aeronautics and Space Administration.

#### REFERENCES

- Barbier, D. 1961, *Planets and Satellites*, edited by G. P. Kuiper (University of Chicago Press, Chicago), Chap. 7.
- Bergh, S. van den. 1962, *Astron. J.* **67**, 147.
- Bullrich, K. 1948, *Ber. Deutsch. Wetterd., U. S.-Zone*, No. 4.
- Diggelen, J. van. 1959, *Rech. Astron. Obs. Utrecht* **14**, No. 2.
- Eimer, M. 1963, *Jet Propulsion Lab., Tech. Rept.* No. 32-347.
- Fedoretz, V. A. 1952, *Publ. Kharkov Obs. 2; Uch. Zap. Kharkov Univ.*, **42**, 49.
- Fessenkov, V. G. 1961, *Physics and Astronomy of the Moon*, edited by Z. Kopal (Academic Press Inc., London), Chap. 4.
- . 1928, *Astron. J. USSR* **5**, 219.
- Johnson, H. L., and Morgan, W. W. 1953, *Astrophys. J.* **117**, 313.
- Kohn, H. W., and Benjamin, B. M. 1961, *American Mineralogist* **46**, 218.
- Minnaert, M. 1961, *Planets and Satellites*, edited by G. P. Kuiper (University of Chicago Press, Chicago), Chap. 6.
- Pohn, H. 1963, *Publ. Astron. Soc. Pacific* **75**, 186.
- Rougier, M. G. 1933, *Ann. Obs. Strasbourg* **2**, 205.
- Shoemaker, E. M., and Hackman, R. J. 1962, *IAU Symp.* No. 14, p. 289.
- Willey, R. L. 1963, *Nature*, **200**, 1056.
- Willstrop, R. V. 1960, *Monthly Notices Roy. Astron. Soc.* **121**, 17.